Serb. Astron. J. № 188 (2014), 45 - 54 **UDC 523.31 – 853 : 523.985.3–73**
DOI: 10.2298/SAJ1488045S Original scientific paper

A COMPARATIVE STUDY OF MEASURED AMPLITUDE AND PHASE PERTURBATIONS OF VLF AND LF RADIO SIGNALS INDUCED BY SOLAR FLARES

D. M. Šulić[1] and V. A. Srećković[2]

[1]*University Union - Nikola Tesla Belgrade, Serbia*
E–mail: *desankasulic@gmail.com*

[2]*Institute of Physics, University of Belgrade, P.O. Box 57, Belgrade, Serbia*
E–mail: *vlada@ipb.ac.rs*

(Received: April 1, 2014; Accepted: May 19, 2014)

SUMMARY: Very Low Frequency (VLF) and Low Frequency (LF) signal perturbations were examined to study ionospheric disturbances induced by solar X-ray flares in order to understand processes involved in propagation of VLF/LF radio signals over short paths and to estimate specific characteristics of each short path. The receiver at the Belgrade station is constantly monitoring the amplitude and phase of a coherent and subionospherically propagating LF signal operated in Sicily NSC at 45.90 kHz, and a VLF signal operated in Isola di Tavolara ICV at 20.27 kHz, with the great circle distances of 953 km and 976 km, respectively. A significant number of similarities between these short paths is a direct result of both transmitters and the receiver's geographic location. The main difference is in transmitter frequencies. From July 2008 to February 2014 there were about 200 events that were chosen for further examination. All selected examples showed that the amplitude and phase of VLF and LF signals were perturbed by solar X-ray flares occurrence. This six-year period covers both minimum and maximum of solar activity. Simultaneous measurement of amplitude and phase of the VLF/LF signals during a solar flare occurrence was applied to evaluate the electron density profile versus altitude, to carry out the function of time over the middle Europe.

Key words. solar-terrestrial relations – Sun: activity – Sun: flares – Sun: X-rays, gamma rays – X-rays: bursts

1. INTRODUCTION

The ionosphere is the part of the atmosphere that contains ionized gases. The primary process is photoionization of thermospheric gases by the Sun's extreme ultraviolet radiation and X-rays. Both these radiations are ~ 100 times stronger at the solar maximum than at solar minimum. Secondary processes include ionization by photoelectrons and scattered or reemitted radiation. The ionosphere, at all latitudes, has a tendency to separate in different regions, despite of the fact that different processes dominate in different latitudinal domains. The regions D, E, and F with two layers F_1 and F_2 are distinct only in the daytime ionosphere at mid-latitudes. The different regions are generally characterized by a density maximum at certain altitude, and density decreases with altitudes on both sides of the maximum.

The lowest region of the ionosphere, the D-region, $50 \leq h \leq 90$ km, is formed primarily by the action of the solar Lyman-alpha radiation (121.6 nm) on nitric oxide. At night, the ionospheric plasma density decreases most rapidly at lower altitudes, and, at 90 km altitude, it decreases from 10^{11} to 10^{8} m^{-3} (Schunk and Nagy 2000).

Very Low Frequency (VLF, 3 - 30 kHz) and Low Frequency (LF, 30 - 300 kHz) radio signals propagate inside the waveguide formed by the lower ionosphere and Earth's surface (Wait and Spies 1964, Mitra 1974). A range of dynamic phenomena occur in the D-region and some of them are: *the diurnal effect (day/night), seasonal effect (summer/winter), correlation with solar activity (sunspot level and solar flares), effects of lightning induced electron precipitation, and red sprites.* All these phenomena are followed by changes in electron density of lower ionosphere, which affects the subionospheric VLF/LF propagation as an anomaly in amplitude and/or phase.

During a solar flare, X-ray irradiances rapidly increase and X-rays with wavelengths below 1 nm are able to penetrate the D-region, causing ionization of the neutral constituents, predominantly nitrogen and oxygen (Mitra 1974).

2. EXPERIMENTAL SETUP

The perturbations in the D-region induced by solar flares, the Sudden Ionospheric Disturbances, (SIDs), were studied using observed amplitude and phase data from VLF/LF transmitters, in the period July 2008 - February 2014. This period of six years includes the minimum and maximum of solar activity. All data were recorded at the Belgrade station (44.85^0 N, 20.38^0 E) by the Stanford University ELF/VLF Receiver Atmospheric Weather Electromagnetic System for Observation Modeling and Education (AWESOME). These data are digitized and saved in two different resolutions - high resolution (50 Hz) and low resolution (1 Hz). Narrowband data can be recorded continuously fashion, even in the case when as many as 15 transmitters are being monitored.

One of the best defined signals received by the AWESOME system at the Belgrade station originates at the NSC transmitter from Sicily Italy at 45.90 kHz. Other signals received at the Belgrade station include: DHO (Germany 23.4 kHz), HWU (France 18.3 kHz), GQD (UK 22.21 kHz), ICV (Italy 20.27 kHz), NRK (Iceland 37.5 kHz), NAA (USA 24 kHz) and NWC (Australia 19.8 kHz). Great circle distances for these signals are in the range from 1 Mm to 12 Mm.

This paper presents the results of short-distance (propagation distance less than 1000 km), subionospherically, VLF/LF propagation for detection of SIDs in the D-region. Locations of the transmitters and the receiving site are presented in Fig. 1. The receiver keeps monitoring the amplitude and phase of coherent and subionospherically propagating VLF signals operated in Sicily (38.00^0 N, 13.50^0 E, NSC at 45.90, kHz) and in Isola di Tavolara (40.88^0 N, 9.68^0 E, ICV at 20.27 kHz), both in Italy, with great circle distances of 953 km and 976 km, respectively. Propagation paths are southwest - northeast oriented. Both signals propagate over sea, ground, sea and ground, which implies very similar conductivity properties of the waveguide bottoms.

Fig. 1. *Great Circle Paths (GCP) of subionospherically propagating VLF signals recorded at the Belgrade station. The receiver is continuously monitoring the amplitude and phase of coherent and subionospherically propagating VLF signals operated in Sicily at 45.90, kHz and Isola di Tavolara at 20.27 kHz.*

For studying solar flare events under similar conditions we have examined only those events that occurred in the time sector for zenith angle $\chi \leq 60^0$. During the local winter and equinox this time sector is between 4 and 5 hours around local noon. Local noon is at 10:50 UT. During the local summer, the time sector lasts about 7 hours. We have already examined around 200 solar flare events and analyzed their effects on propagation characteristics of VLF/LF signals.

This work deals with a typical X-ray irradiance I_X[Wm^{-2}] recorded by GOES - 15 satellite for wavelengths ranging from 0.1 to 0.8 nm, available from USA National Oceanic and Atmospheric Administration (NOAA) via the web site: www.swpc.noaa.gov/ftpmenu/lists/xray.html.

3. MEASURED DATA

The time stability of NSC transmitter enabled continuous day and night monitoring not only the amplitude but also the phase. Fig. 2 shows diurnal variations of amplitude (upper panel) and phase (lower panel) of NSC/45.90 kHz signal against the universal time (UT), recorded by the AWESOME system at the Belgrade station on May 4, 2012. Moments of sunrise and sunset for the receiver site and the NSC transmitter are labeled by vertical lines in Fig. 2, respectively.

The diurnal change of phase is characterized by the midday peak and the amplitude has bigger values during night than in daytime condition because of lower absorption. Taking into consideration the measured data shown in Fig. 2 it is possible to follow the nighttime, sunrise, daytime, sunset and again nighttime propagation conditions.

3.1. Perturbations of VLF/LF radio signals by solar X-ray flare

Simultaneous observations of amplitude (A) and phase (Φ) in VLF/LF signals during solar flares could be applied to calculations of electron density profile. Therefore, the perturbation of amplitude was estimated as a difference between values of the disturbed amplitude induced by flare and amplitude during the normal condition in the D-region: $\Delta A = A_{\rm dis} - A_{\rm nor}$, where dis means the disturbed and nor means normal condition. In the same way the perturbation of phase was estimated as: $\Delta\Phi = \Phi_{\rm dis} - \Phi_{\rm nor}$.

Among 200 events of amplitude and phase perturbations on ICV/20.27 kHz and NSC/45.90 signals recorded at the Belgrade station there is one induced by a minor B8.8 class solar flare and one induced by an extremely large X1.44 class solar flare. This large solar flare occurred on July 12, 2012 with maximum at 16:49 UT. All other examined perturbations of amplitude and phase on ICV/20.27 kHz and NSC/45.90 kHz signals were induced by small and moderate solar flares.

On November 3, 2008 B8.8 a class solar X-ray flare occurred with maximum at 10:20 UT. Although B-flares are considered minor, the blast nevertheless made itself felt in the D-region. Fig. 3a shows the time variation of X-ray irradiance, measured disturbances in amplitude and phase (ΔA and $\Delta\Phi$) on ICV/ 20.27 kHz and NSC/45.90 kHz signals recorded at the Belgrade station. The upper panel time variation shows the of X-ray irradiance. Disturbances in amplitude and phase of both signals caused by the solar X-ray flare are shown in the middle

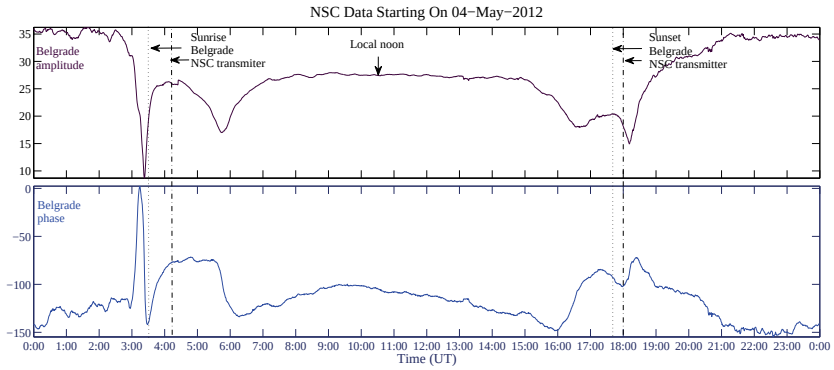

Fig. 2. *The amplitude (upper panel) and phase (lower panel) as a function of universal time of NSC/45.90 kHz signal, as recorded at Belgrade on May 4, 2012.*

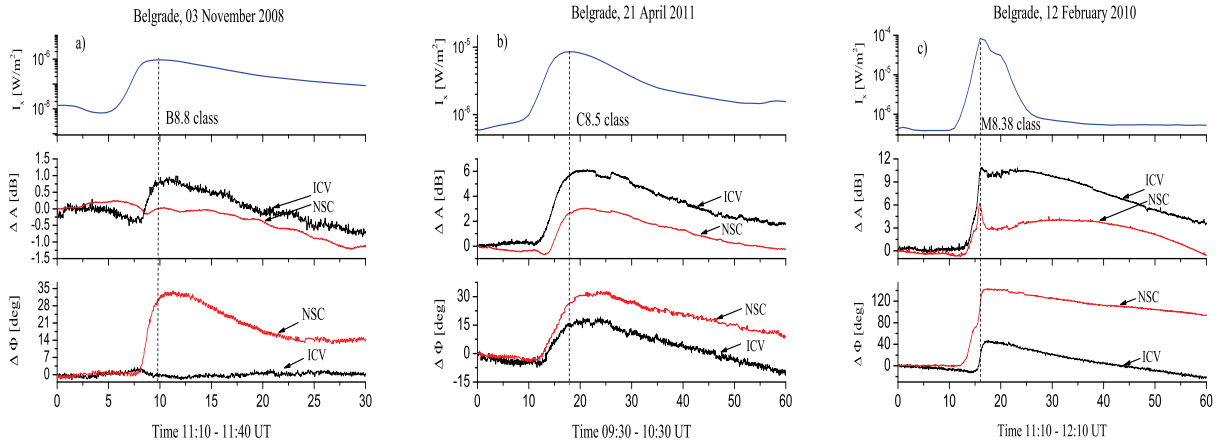

Fig. 3. *Perturbations of amplitude and phase on NSC/45.90 kHz and ICV/20.27 kHz signals recorded at the Belgrade station during a minor* ***B8.8*** *class solar flare, small* ***C8.5*** *class solar flare and medium* ***M8.38*** *class solar flare, as shown in panels a), b) and c), respectively.*

and lower panel, respectively. The perturbation of amplitude of the ICV/20.27 kHz signal caused an increase of $\Delta A = 0.9$ dB. There was no evidence of a perturbation in phase. There was no recorded perturbation of amplitude in the NSC/45.90 kHz signal, while at the same time the phase increased by $\Delta\Phi \sim 30^0$. Detecting a minor B8.8 flare is a good test of the method sensitivity for monitoring of the the solar activity. Also, it is the first evidence of the amplitude and phase sensitivity to solar flare depending on the transmitter frequency.

In Fig. 3b there are the X-ray irradiance, and perturbations of amplitude and phase on ICV/20.27 kHz and NSC/45.90 kHz signals during a small C8.5 class solar flare on April 21, 2011. For this, a bit stronger flare, additional ionization in the D-region causes disturbances of both the amplitude and phase signals of ICV/20.27 kHz and NSC/45.90 kHz. As presented in Fig. 3b, the shapes of perturbed amplitude (middle panel) and phase (lower panel) on VLF and LF signals are very similar to each other. This similarity can be identified in all disturbances of ICV/20.27 kHz and NSC/45.90 kHz signals caused by small solar flares.

On February 12, 2010, a M8.38 class solar flare occurred with maximum intensity of $I_X = 8.38 \cdot 10^{-5}$ W/m^2 at 11:26 UT producing an intensive SID. Fig. 3c shows the time variation of X-ray irradiance (upper panel). Measured disturbances in amplitude and phase of ICV/20.27 kHz and NSC/45.90 kHz signals are presented in the middle and lower panels of Fig. 3c. The increase of amplitude of ICV/20.27 kHz was very high and, at its maximum, it had value higher by 10.3 dB with respect to the normal level before the beginning of the solar flare. Simultaneously, the phase of the signal was disturbed with the maximum increase of $\Delta\Phi = 44^0$. The intensity of X-ray suddenly increased and, after reaching a maximum, slowly decreased. At the same time, the amplitude of NSC/45.90 kHz signal passed through a peak and, a few minutes after the moment of the maximum intensity X- ray amplitude, it is slowly increased again to another peak. The disturbance of phase was manifested by the increase of $\Delta\Phi = 138^0$ at 10:28 UT and, after that, it slowly decreased to its normal daytime level.

Table 1 provides numerical values of perturbations of amplitude and phase on ICV/20.27 kHz and NSC/40.95 kHz signals recorded at the Belgrade station induced by different solar X-ray flare types.

In all the examined events, the amplitude of the ICV/20.27 kHz signal is more sensitive than the phase due to the SIDs (see, e.g. Fig. 3). Fig. 4a shows the measured excess of perturbation amplitude, $\Delta A = A_{\rm dis} - A_{\rm nor}$, on ICV/20.27 kHz signal recorded at the Belgrade station as a function of the X-ray irradiance. The examined events were recorded in time sector for the zenith angle $\chi \leq 60^0$. In Fig. 4, dots present the measured ΔA during small and moderate solar X-ray flares. The measured excess of amplitude has value $1 \leq \Delta A \leq 10$. Fig. 4a shows that ΔA is nearly proportional to the logarithm of the X-ray irradiance maximum, with the Adjusted R-Square and Pearson's r coefficients equal to 0.83 and 0.91, respectively.

The measured excesses of amplitude ΔA of the ICV/20.27 kHz signal induced by moderate solar X-ray flares are larger then ΔA of GQD/20.21 kHz and NAA/24.0 kHz signals also recorded at the Belgrade station. The VLF signal propagates from the GQD transmitter to the receiver site over the great circle distance of 2000 km and the VLF signal emitted from the NAA transmitter propagates to the receiver site over the great circle distance of 6560 km. The results on propagation characteristics and perturbations amplitude and phase of these VLF signals are published by Zigman et al. (2007) and Grubor et al. (2008).

The flare induced phase perturbations always increase on the ICV/20.27 kHz signal.

As we pointed out in this paper, the best defined amplitude and phase of signal received by the AWESOME system at the Belgrade station originates from the NSC transmitter in Sicily, Italy at 45.90 kHz. This LF signal propagates over the great circle distance of 952 km. Perturbations of amplitude are not well defined during solar flare occurrences with X-ray irradiances less than irradiance corresponding to the C3 class solar flare. The measured amplitude excess amounts to $-0.6 \leq \Delta A \leq 1$ dB. In Fig. 4b, squares present the measured ΔA during small and moderate solar X-ray flares. Solar

Table 1. Numerical values of perturbations of amplitude and phase on VLF and LF signals induced by different solar flares

	Minor solar flare **B8.8** class $I_X = 8.8 \cdot 10^{-7}$ [W/m^2]		Small solar flare **C8.5** class $I_X = 8.5 \cdot 10^{-6}$ [W/m^2]		Moderate solar flare **M8.38** class $I_X = 8.38 \cdot 10^{-5}$ [W/m^2]	
	ΔA [dB]	$\Delta\Phi$ [deg]	ΔA [dB]	$\Delta\Phi$ [deg]	ΔA [dB]	$\Delta\Phi$ [deg]
ICV/20.27 kHz	0.9	0^0	6.2	15^0	10.3	44^0
NSC/45.90 kHz	0	30^0	3.76	40^0	6.63	138^0

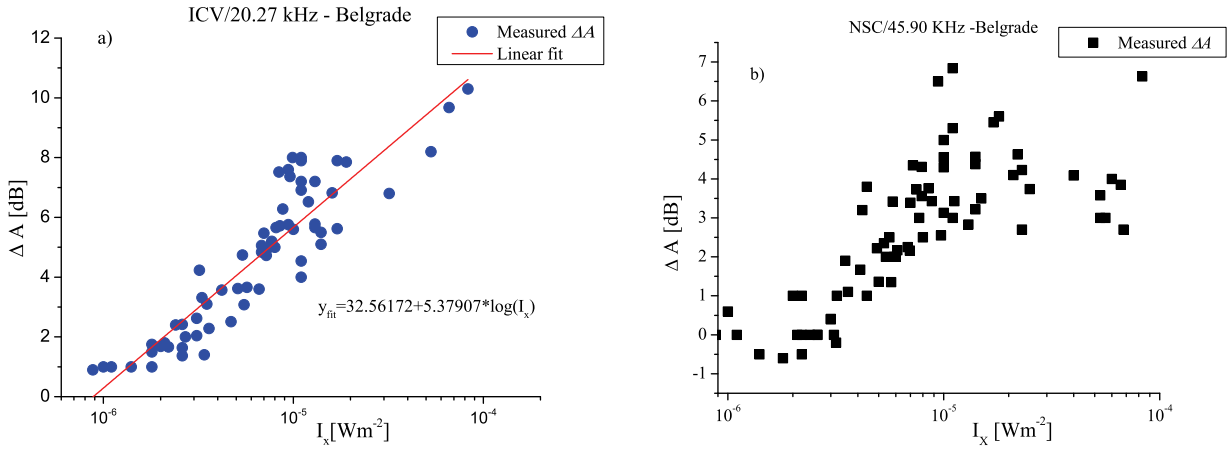

Fig. 4. *a) Measured excesses of perturbation amplitude of ICV/20.27 kHz signal as a function of solar X-ray irradiance, and b) Measured excesses of perturbation amplitude on NSC/45.90 kHz signal as a function of solar X- ray irradiance.*

flares from the C3 class to approximately M2 class caused perturbations of amplitude and phase of signal. Variation of the perturbed amplitude in time is very similar to the time variation of the X-ray irradiance. The result of our study is that solar flares larger than the M2 class induced such perturbation of amplitude that oscillates around the level of before the beginning of the flare. The amplitude is perturbed in such a way that it passes through a peak and then trough the next peak, etc. In all examples that we analyzed, the amplitude reaches the first peak in time close to the maximum intensity of the solar X-ray flare. After that, the amplitude decreases during the next few minutes reaching the minimum. This is the consequence of the complicated nature of physical processes in the perturbed D-region and LF signal propagation.

The recorded phase of the NSC signal is very sensitive to SIDs induced by a solar X-ray flare. The perturbation of the signal phase has a time variation which is very similar to the time variation of the solar flare irradiance. An increase of phase induced by a small solar X-ray flare reached a maximum at time that is very close to time of the maximum intensity of the solar flare. When a moderate solar X-ray flare induces disturbances in the D-region, the time of phase maximum is few minutes after the moment of the maximum intensity of the solar X-ray flare.

3.2. Reproducibility of the measured amplitude perturbations.

Solar flare affects the recorded VLF/LF signal amplitude and phase. The stability and reproducibility of the received amplitude and phase of the NSC/45.90 kHz signal were found in many examined events recorded during the period of six years. To illustrate this, Fig. 5a provides time variation of perturbed amplitudes affected by two C class solar flares that occurred about a year apart. One solar flare occurred on May 5, 2010 with the peak irradiance $I_X = 8.8 \cdot 10^{-6}$ W/m^2, and the other on April 21, 2011 with the peak irradiance $I_X = 8.5 \cdot 10^{-6}$ W/m^2. Time variations of the perturbed amplitude A and amplitude excess ΔA for these two events have almost identical shapes and, as can be seen, even the values are very similar.

Fig. 5b shows reproducibility of amplitude perturbations affected by the M class solar flares. On July 2, 2012, there was a flare with a peak irradiance $I_X = 5.6 \cdot 10^{-5}$ W/m^2 and on March 8, 2011 the flare with a peak irradiance of $I_X = 5.3 \cdot 10^{-5}$ W/m^2 was recorded. Both of them affected the amplitudes. Time variations of perturbed amplitude for these two events have very similar shapes.

Similar level of X-ray irradiances makes changes in the lower ionosphere, which also similarly influences the characteristics of the subionospheric VLF/LF propagation by causing an increase in amplitudes. This reproducibility and their sensitivity make propagation of VLF/LF signals a useful and reliable tool in evaluating electron density in the D-region.

4. METHOD OF SIMULATION: APPLICATION TO SOLAR FLARE INDUCED PERTURBATIONS OF VLF/LF RADIO SIGNALS

Radio signals in VLF and LF ranges propagate from transmitters through a waveguide bounded by the Earth's surface and the D-region. This propagation is stable both in amplitude and phase and has a relatively low attenuation. Characteristics of the D-region have a strong influence on propagation of VLF/LF signals. Theoretical base for this propagation under normal, undisturbed, ionospheric conditions is developed by Wait and Spies (1964). The influence of the D-region is taken into account by using the so called Wait's parameters: the sharpness β (km^{-1}) and the reflection height h'(km). The Naval Ocean System Center, San Diego, USA has developed a computer program, the LWPC- Long Wave Propagation Capability, for simulation of VLF/LF

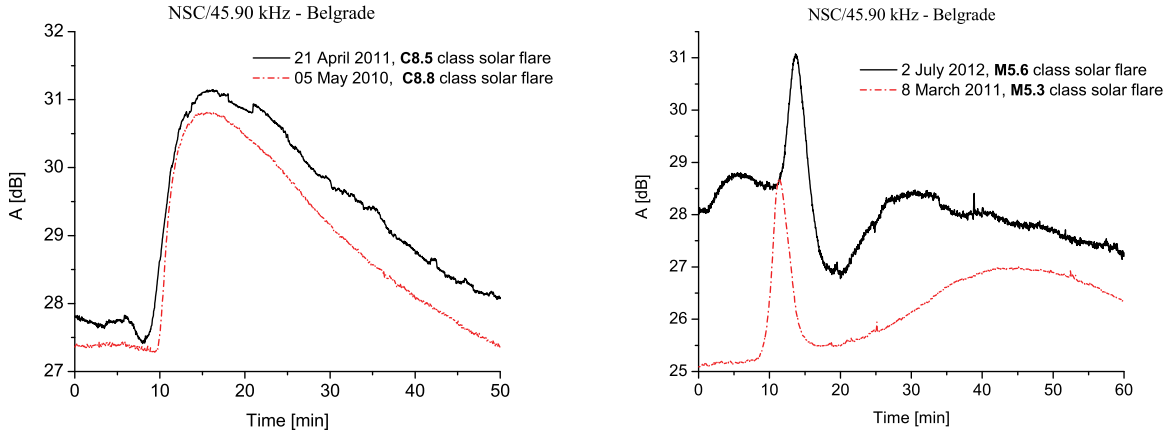

Fig. 5. *Reproducibility of measured amplitude perturbations. Parallel presentation of two events of amplitude perturbation of signal NSC/45.90 kHz versus time: a) induced by two C class flares which occurred on May 05, 2010 and April 21, 2011; b) induced by two M class flares, occurred on July 2, 2012 and March 8, 2011.*

propagation along any particular great circle path under different diurnal, seasonal and solar cycle variations in the ionosphere (Ferguson 1998). The LWPC program can take arbitrary electron density versus altitude profiles supplied by the user to describe the D-region and thus the ceiling of the waveguide.

The Wait's parameters were used successfully to calculate the electron density height profiles in the D-region under the regular change of day/night and season or solar cycle variation (Thomson 1993, Thomson and Clilverd 2001, McRae and Thomson 2000). A very remarkable change in the electron density is caused by solar X-ray flares, so the Wait's parameters were used in calculations of the electron density height profiles in a suddenly disturbed D-region, (Thomson and Clilverd 2001, Thomson 2005, Zigman et al. 2007, Nina et al. 2011, 2012a,b, Šulić et al. 2010, Grubor et al. 2008).

A convenient quantity to describe the characteristics of the D-region is based on a *height dependent conductivity parameter*, $\omega_r(h)$. Wait and Spies defined this quantity as: $\omega_r(h) = \omega_p^2(h)/\nu(h) = 2.5{\cdot}10^5{\cdot}e^{\beta\cdot(h-h')}$ where ω_p is the electron plasma frequency (angular) and $\nu(h)$ is the effective electron-neutral collision frequency, both being functions of height h in km. This definition assumes that $\omega_r(h)$ varies exponentially with height at rate determined by the constant $\beta(\mathrm{km}^{-1})$. h' is the height (km) at which $\omega_r(h) = 2.5 \cdot 10^5$ rad/s and has been found to be a convenient measure for the "reflection height" of the ionosphere (Wait and Spies 1964). The electron density profile increases exponentially with height and can be associated with the above defined equations. The equation for the electron density in the D-region:

$$N_e(h,t) = 1.43{\cdot}10^{13} e^{0.15h'(t)} e^{(\beta(t)-0.15)\cdot(h-h'(t))} \quad \mathrm{m}^{-3}, \tag{1}$$

was derived by Thomson (1993) and we also use it in our work to calculate the vertical density profile in the range 50 - 90 km.

Typically, the electron density profile is changing from day to day even during magnetically quiet periods. Our intention was to calculate the electron density profile versus height, and versus time. To estimate sharpness β and reflection height h' for normal condition in the daytime D-region we used the following formulas below derived by Ferguson:

$$\beta_0 = 0.5349 - 0.1658\cos\chi - 0.08584{\cdot} \cdot\cos\varphi + 0.1296X_5 \quad \mathrm{km}^{-1} \tag{2}$$

$$h'_0 = 74.37 - 8.087\cos\chi + 5.779\cos\theta - 1.213\cos\varphi - 0.0044X_4 - 6.035X_5 \quad \mathrm{km}. \tag{3}$$

Here χ is the solar zenith angle, θ is the geographical latitude, $\varphi = 2\pi(m-0.5)/12$, m is the ordinal number of month in the year, X_4 is the Zurich sunspot number and $X_5 = 0$ or 1 for magnetically quiet or disturbed conditions, respectively (Ferguson 1980)

The first step of the *trial and error method* used is the simulation of VLF/LF signals propagating from the transmitter to the receiver site under the normal ionospheric condition in the D-region and estimation of the initial sharpness β_0 and reflection height h'_0 by Eqs. (1) and (2). Using the LWPC program with these Wait's parameters we simulated the propagation of VLF/LF signals and obtained the simulated values for the amplitude and phase.

The next step is to simulate the propagation of VLF/LF signals through the waveguide while the D-region was disturbed for the characteristic moments during the flare development. We choose the next pair of β and h' and used it as input parameter in the LWPC program to obtain the simulated values of amplitude and phase at the receiver site.

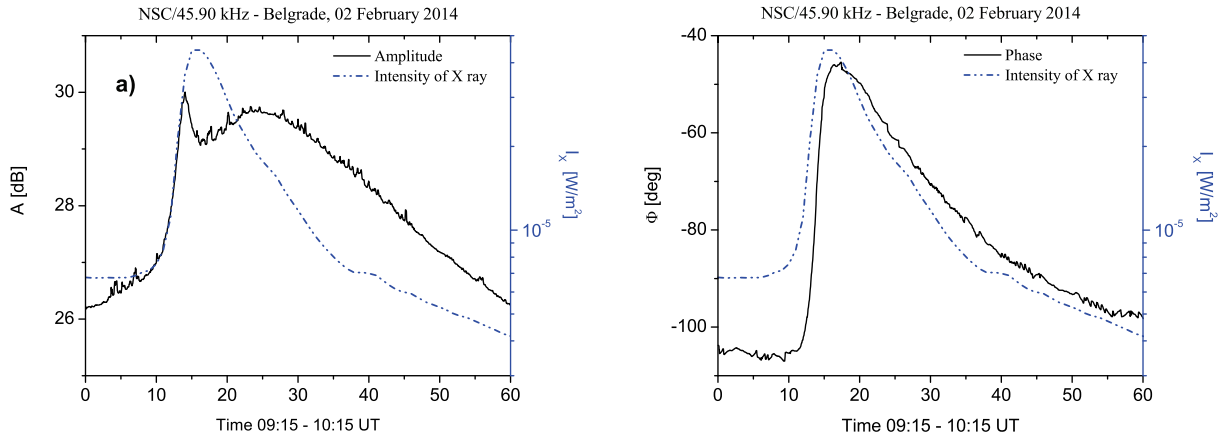

Fig. 6. *The time variation of the X-ray irradiance measured by the GOES-15 satellite (dash - dot - dot), and the perturbed amplitude and phase of the signal emitted from the NSC transmitter and recorded by the AWESOME receiver in Belgrade (Serbia) during the observed M4.46 class solar flare (from 09:15 to 10:15 UT) on February 2, 2014.*

The process was repeated until differences between the simulated amplitudes and phases for the disturbed and normal condition in the D-region matched the measured ones ΔA and $\Delta\Phi$, respectively. After achieving a good matching: $\Delta A_{\rm sim} \approx \Delta A$ and $\Delta\Phi_{\rm sim} \approx \Delta\Phi$, the corresponding pair of β and h' was used for calculation of the electron density versus height for characteristic moments during and after the solar flare occurrence. In the above expressions the index "sim" stands for "simulated".

4.1. Example of an electron density profile in the perturbed D-region

On February 2, 2014, seventeen solar flares occurred. In this paper we present results for the perturbed electron density in the D-region induced by a M4.4 class solar flare with the peak irradiance $I_X = 4.46 \cdot 10^{-5}$ Wm^{-2} that took place at 09:31 UT. This flare event caused disturbances of the amplitude and phase of the NSC/45.90 signal as evident from plots given in Fig. 6. Fig. 6a gives the X-ray irradiance and the observed perturbation amplitude of the LF signal versus the universal time. As the X-ray irradiance increased, it caused an increase of amplitude till 09:29 UT when the amplitude decrease began. Within the time interval 09:29 - 09:32 UT the amplitude passed through a minimum. This time interval corresponds to the time of the X-ray peak irradiance. Sudden disturbances in the D-region changed propagation characteristics of the LF radio signal, which resulted in signal attenuation.

Fig. 6b shows the time variation of the X-ray irradiance and the measured phase of the signal for the time interval 09:15 - 10:15 UT. This time variation of the perturbed phase is in close correlation with time variation of the X-ray irradiance. The maximum of the perturbed phase occurred at 09:32 UT, lasted one minute after the appearance of the X-ray peak irradiance.

One of the objectives of this work was to calculate the electron profile as a function of time, during and after the occurrence of solar flare. In accordance to this, it was necessary to obtain $\beta(t)$ and $h'(t)$ for the entire examined time interval and used them as input parameters for the LWPC program.

Table 2 contains measured values ΔA, $\Delta\Phi$, together with quantities obtained by the LWPC program: the sharpness, β, reflection height h' and electron density $N_{\rm e}$ at the referent height $h = 70$ km all these for different instants during the M4.46 class solar flare occurrence and the recovery period. The X-ray irradiance $I_X = 4.26{\cdot}10^{-5}$ Wm^{-2} at 09:32 UT induced amplitude and phase perturbations of $\Delta A = 3.05$ dB and $\Delta\Phi = 58^0$, respectively. We obtained for the sharpness $\beta = 0.357$ km^{-1} and for reflection height $h' = 64.55$ km which means that the reflection height was lowered by 5.45 km. The electron density increased at $h = 70$ km from $3.94{\cdot}10^8$ m^{-3} to $2.76{\cdot}10^9$ m^{-3}.

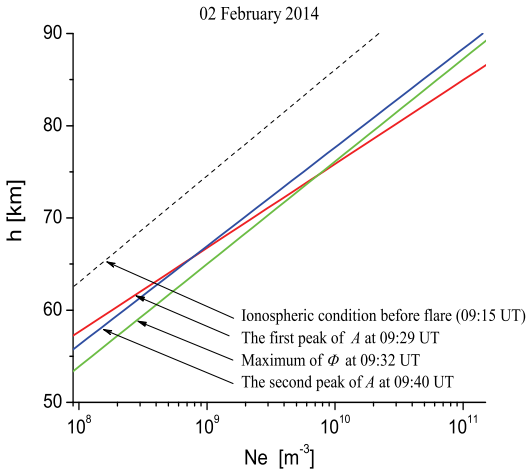

Fig. 7. *The flare time electron densities for values of β and h' given in Table 2 (the height profile of electron density).*

Table 2. Values of the measured amplitude and phase perturbations, and evaluated quantities β and h', and electron densities N_e (at h=70km) for different instants during and after the occurrence of the M4.46 class solar flare.

Time [UT]	I_X [10^{-5} Wm^{-2}]	NSC/45.90 kHz				
		ΔA [dB]	$\Delta\Phi$ [deg]	β [km^{-1}]	h' [km]	N_e [10^9m^{-3}]
09:15	0.677	-	-	0.350	70.00	0.39
09:24	1.900	0.60	-3	0.380	69.20	0.53
09:27	1.550	1.25	28	0.397	68.20	0.80
09:29	3.600	3.65	32	0.403	65.70	2.20
09:32	4.260	3.05	58	0.357	64.55	2.76
09:35	2.950	3.24	54	0.358	64.90	2.40
09:40	1.770	3.42	42	0.365	65.70	1.89
09:45	1.800	3.18	33	0.362	66.55	1.37
09:50	0.803	2.57	26	0.359	67.30	1.04
09:55	0.699	2.08	18	0.352	68.15	0.76
10:00	0.599	1.51	14	0.352	68.65	0.63
10:05	0.529	0.96	10	0.350	69.04	0.55
10:10	0.283	0.48	6	0.350	69.50	0.47

Fig. 7 shows the vertical electron density profile before and during the M4.46 class solar flare of February 2, 2014. So, there is the vertical electron density profile before the beginning of the flare (09:15UT), for the characteristic moments when the amplitude passed through the first and the second peak, and the phase after passing the maximum. The corresponding electron density profiles moved to higher electron densities with different slopes as compared to the density profile of the ionospheric condition existing prior the flare start.

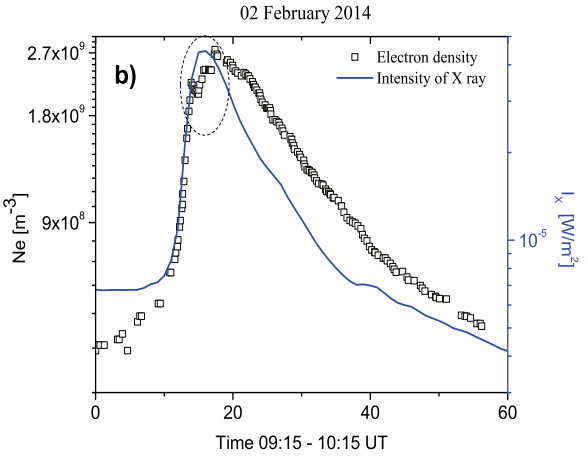

Fig. 8. *Variation of the X-ray irradiance, as measured by the GOES-15 satellite, and the corresponding electron density evaluated at the height of 70 km versus the universal time. The electron density profile is obtained from measured perturbed amplitude and phase of the NSC/45.90 kHz signal at the Belgrade station.*

Fig. 8 shows simultaneously the X-ray irradiance and calculated electron density (at the reference height $h = 70$ km) as a function of time (for the interval 09:15UT - 10:15UT). The oval marks values of the electron density based on the values of the attenuated amplitude after the first peak presented in Fig. 6a. It can be noticed that the time distribution of the electron concentration follows the variation with time of the registered solar flux on the GOES-15 satellite.

5. DISCUSSION AND CONCLUSION

The purpose of this work was to examine perturbations of amplitude and phase on VLF/LF radio signals propagating over the great circle path with distances smaller than 1000 km, the so called short path. The receiver at the Belgrade station continuously monitors the amplitude and phase of coherent and subionospherically propagating radio signals operated in Sicily, NSC at 45.90 kHz and in Isola di Tavolara, ICV at 20.27 kHz, with great circle distances of 953 km and 976 km, respectively. Geographically and in accordance to conductivity properties, these two short paths are very similar to each other. The main difference is in the transmitter frequency, and for this reason, a detailed study was done around of 200 events of SID and of their influence to amplitude and phase on ICV/20.27 kHz and NSC/45.90 kHz signals (see Fig. 4). Measured data were obtained over a period of six years covering the minimum and maximum of solar activity.

Our first conclusion is that the amplitude of the ICV/20.37 kHz signal is more sensitive to the disturbances caused by the X-ray solar flare than the phase. In all events the increasing X-ray irradiance induced an increase of the amplitude and phase. It was shown that the difference between the perturbed and normal amplitude changed from $\Delta A = 1$dB up to $\Delta A = 10$ dB. Fig. 4a shows a monotonous logarithmic increase of ΔA with the solar X-ray irradiance (ΔA is nearly proportional to the logarithm of I_x).

Analyzing propagation characteristics of the NSC/45.90 kHz signal and the perturbed amplitude and phase caused by the solar X-ray flare we are able to make the following conclusions:

Perturbations of phase on the NSC/45.90 kHz signal are very pronounced. A minor solar flare, like the B8.8 class, induced a phase increase, $\Delta\Phi \sim 30^0$. The time variation profile of perturbed phase is very similar of the X-ray irradiance.

During the occurrence of solar flares, classified as a minor and small flare up to the C3 class, the amplitude of the signal NSC/45.90 kHz does not have significant perturbations. A solar flare in the range from C3 to M3 classes induced an increase of the signal amplitude. Moderate solar flares, classified larger then the M3 class, induced an oscillation of amplitude around the base level existing before the beginning of the flare (Fig. 5b).

The stability and reproducibility of the received amplitude and phase of the NSC/45.90 kHz signal were found in many examined events recorded during the six year period. This is illustrated in Figs. 5a and 5b. This reproducibility gives the possibility that only by looking into the measured data, we are able to define the class of the perturbing solar X-ray flare.

As the presence of electrons in the ionospheric D-region strongly affects the VLF/LF radio wave propagation we present a method for determination of the electron density. Using the measured ΔA and $\Delta\Phi$ as very important quantities and the LWPC program, we calculated the electron density in the D-region. Also, it is possible to calculate the electron density profile as a function of time, to follow its increase during the time interval of the peak irradiance, and to study the decrease of the electron density during the recovery period.

It can be noticed that the time distribution of the electron density follows the time variation pattern of the registered solar flux on the GOES-15 satellite. In the case analyzed, the electron concentration (at the reference height) has values within an order of magnitude, 10^8 - 10^9 m^{-3}, during the observed flare (see Table 2). Finally, we can see (Fig. 7) that the considered solar flare, as expected, causes larger increases in electron concentration at higher altitudes.

Acknowledgements – The authors are very grateful to colleagues from the AOB, especially to Zorica Cvetković for a very fruitful discussion. Also, the authors are thankful to the Ministry of Education, Science and Technological Development of the Republic of Serbia for support of this work within projects 176002 and III4402.

REFERENCES

Ferguson, J. A.: 1980, in "Ionospheric profiles for predicting nighttime VLF.LF propagation, Naval Ocean Systems Center Tech. Rept NOSC/TR 530", NTIS Accession No ADA085399, National Technical Informations Service Springfield, VA 22161, U.S.A.

Ferguson, A. J.: 1998, in "Computer Programs for Assessment of Long- Wavelength Radio Communications, Version 2.0, Technical document 3030", Space and Naval Warfare Systems Center, San Diego CA 92152-5001.

Grubor, D. P., Šulić, D. and Žigman, V.: 2008, *Ann. Geophys.*, **26**, 1731.

McRae, M. W. and Thomson, N. R.: 2000, *J. Atmos. Sol.-Terr. Phys.*, **62**, 609.

Mitra, A. P.: 1974, in "Ionospheric Effects of Solar Flares." eds. D. Reidel, Dordrecht, Holland.

Nina, A., Čadež, V., Srećković, V. A. and Šulić, D.: 2011, *Balt. Astron.*, **20**, 609.

Nina, A., Čadež, V., Srećković, V. and Šulić, D.: 2012, *Nucl. Instrum. Meth. B*, **279**, 110.

Nina, A., Čadež, V., Šulić, D., Srećković, V. and Zigman, V.: 2012, *Nucl. Instrum. Meth. B*, **279**, 106.

Schunk, R. W. and Nagy, A. F.: 2000, in "Ionospheres: physics, plasma physics and chemistry", Cambridge University Press, 570.

Šulić, D., Nina A., Srećković, V.: 2010, *Publ. Astron. Obs. Belgrade*, **89**, 391.

Thomson, N. R.: 1993, *J. Atmos. Sol.-Terr. Phys.*, **55(2)**, 173.

Thomson, N. R., Rodger, C. J. and Clilverd, M. A.: 2000, *J. Geophys. Res.* **110**, A06306.

Thomson, N. R. and Clilverd, A. M.: 2001, *J. Atmos. Sol.-Terr. Phys.*, **63**, 1729.

Wait, J. R. and Spies, K. P.: 1964, in "Characteristics of the Earth-ionosphere waveguide for VLF radio waves, Technical Note 300", National Bureau of Standards, Boulder, CO.

Žigman, V., Grubor, D. and Šulić, D.: 2007, *J. Atmos. Sol.-Terr. Phys.*, **69(7)**, 775.

УПОРЕДНА АНАЛИЗА ПОРЕМЕЋАЈА АМПЛИТУДЕ И ФАЗЕ РАДИО-СИГНАЛА ВРЛО НИСКИХ И НИСКИХ ФРЕКВЕНЦИЈА У ТОКУ ПОЈАВЕ СУНЧЕВЕ ЕРУПЦИЈЕ

D. M Šulić[1] and V. A. Srećković[2]

[1]*University Union - Nikola Tesla Belgrade, Serbia*
E–mail: *desankasulic@gmail.com*

[2]*Institute of Physics, University of Belgrade, P.O. Box 57, Belgrade, Serbia*
E–mail: *vlada@ipb.ac.rs*

УДК 523.31 – 853 : 523.985.3–73
Оригинални научни рад

Поремећаји амплитуде и фазе радио-сигнала врло ниских (VLF, 3 - 30 kHz) и/или ниских фреквенција, (LF, 30 - 300 kHz) који су последица наглог пораста интензитета X-зрачења у току Сунчеве ерупције, проучавани су у циљу одређивања услова простирања радио-сигнала у D-области јоносфере. У току наглог и интензивног пораста X-зрачења долази до пораста густине електрона у D-области јоносфере. У Београду је инсталисана станица AWESOME јуна 2008. године, која континуирано региструје амплитуде и фазе радио-сигнала у наведеним фреквенционим опсезима, а исте емитују предајници распоређени на различитим локацијама у свету. У овом раду приказани су резултати проучавања поремећаја амплитуде и фазе ICV/20.27 kHz радио-сигнала који емитује предајник у Isola di Tavolara и NSC/45.90 kHz радио-сигнала емитованог са предајника на Сицилији (оба се налазе у Италији). VLF/LF радио-сигнали се простиру кроз таласовод чија је доња гранична област површина Земље а горња D-област јоносфере. У временском периоду од јуна 2008. до фебруара 2014. године изабрано је око 200 догађаја у току којих је дошло до наглог пораста интензитета X-зрачења. Наведени шестогодишњи период обухвата минимум и максимум Сунчеве активности). Наглашавамо да су то биле Сунчеве ерупције класификоване као мале C и умерене M ерупције. Одређивање степена пораста амплитуде и фазе VLF/LF радио-сигнала у току Сунчеве ерупције користили смо за одређивање промене густине електрона у функцији висине у D-области јоносфере, као и за одређивање густине електрона на задатој висини у функцији времена пре, у току и после појаве Сунчеве ерупције.